Supporting Information

Single-Atom Cu-N_2 Catalyst Eliminates Oxygen Interference for Electrochemical Sensing of Hydrogen Peroxide in Living Animals

Xiaolong Gao,[ac]‡ Wenjie Ma,[ac]‡ Junjie Mao,[d]‡ Chunting He,[e] Wenliang Ji,[a] Zheng Chen,[d] Wenxing Chen,[f] Wenjie Wu,[a] Ping Yu,[ac] and Lanqun Mao*[abc]

[a] Beijing National Laboratory for Molecular Sciences, Key Laboratory of Analytical Chemistry for Living Biosystems, Institute of Chemistry, The Chinese Academy of Sciences (CAS), Beijing 100190, China

[b] College of Chemistry, Beijing Normal University, Xinjiekouwai Street 19, Beijing 100875, China

[c] University of Chinese Academy of Sciences, Beijing 100049, China

[d] Key Laboratory of Functional Molecular Solids, Ministry of Education, College of Chemistry and Materials Science, Anhui Normal University, Wuhu 241002, China

[e] MOE Key Laboratory of Functional Small Organic Molecule, College of Chemistry and Chemical Engineering, Jiangxi Normal University, Nanchang 330022, China

[f] Beijing Key Laboratory of Construction Tailorable Advanced Functional Materials and Green Applications, School of Materials Science and Engineering, Beijing Institute of Technology, Beijing 100081, China

‡ These authors contributed equally to this work.

* Email: lqmao@bnu.edu.cn

Table of contents

1. Materials and Methods

Materials. Copper (II) nitrate hydrate [$Cu(NO_3)_2$•$3H_2O$], iron (III) nitrate nonahydrate [$Fe(NO_3)_3$•$9H_2O$], cobalt (II) nitrate hexahydrate [$Co(NO_3)_2$•$6H_2O$], manganese (II) acetate [$Mn(CH_3COO)_2$] and ethanol were purchased from Sinopharm Chemical Reagent Co. Ltd. (Shanghai, China). LUDOX® AS-40 colloidal silica, dopamine (DA), uric acid (UA), 3,4-dihydroxyphenylacetic acid (DOPAC), 5-hydroxytryptamine (5-HT), mercaptosuccinate (MCS), and glutathione monoethyl ester (GSOEt) were purchased from Sigma-Aldrich. Cyanamide, ammonium bifluoride (NH_4HF_2) were purchased from Alfa Aesar. The water used in all experiments was ultrapure (18.2 MΩ•cm). Carbon nanotubes (CNTs, single-walled, 5-15 μm in length and 1-2 nm in diameter) was purchased from Shenzhen Nanotech Co., Ltd. (Shenzhen, China). All chemical regents were used as supplied without further purification. Artificial cerebrospinal fluid (aCSF) used as the electrolyte for *in vitro* and *in vivo* electrochemical measurements was prepared by mixing NaCl (126 mM), KCl (2.4 mM), KH_2PO_4 (0.5 mM), $MgCl_2$ (0.85 mM), $NaHCO_3$ (27.5 mM), Na_2SO_4 (0.5 mM), and $CaCl_2$ (1.1 mM) into water and then adjusting the pH to 7.4.

Synthesis of C_3N_4. C_3N_4 was synthesized with a slightly modified method according to the previous literature.[1] Briefly, cyanamide (5 g) and LUDOX® AS-40 silica dispersion (12.5g) were mixed together until the suspension turned to apparent. The mixture was heated at 100 °C for several hours upon stirring to the formation of a white solid. The white powder was then grounded in a mortar, transferred into a crucible and heated up to 550 °C with the heating rate of 2.3 °C•min^{-1} and then kept at 550 °C for 4 h under air. The as-obtained yellow powder was grounded in a mortar and then treated with a 4 M NH_4HF_2 solution under stirring for 2 days. The precipitate was obtained after filtration, washed with distilled water and ethanol for several times. The resultant yellow solid was dried under vacuum at 120 °C overnight.

Synthesis of Cu_1/C_3N_4. The Cu_1/C_3N_4 was synthesized by adding $Cu(NO_3)_2$ solution (10 mg•mL^{-1}) to the C_3N_4 dispersion (4 mg•mL^{-1}). After stirring for about 24 h, the suspension was centrifuged, and the precipitate was washed with water and ethanol for several times and finally dried under vacuum at 70 °C. The as-prepared powder was transferred into a ceramic boat and then placed into a tube furnace. The sample was heated to 400 °C with a heating rate of 3 °C•min^{-1} and kept at 400 °C for 2 h under 5% H_2/Ar atmosphere.

The Fe_1/C_3N_4, Co_1/C_3N_4 and Mn_1/C_3N_4 catalysts were prepared using the similar procedure with the Cu_1/C_3N_4 catalyst except for replacing copper salt with $Fe(NO_3)_3$•$9H_2O$, $Co(NO_3)_2$•$6H_2O$ and $Mn(CH_3COO)_2$, respectively.

Preparation of Cu_1/C_3N_4/CNT. 1 mg•mL^{-1} Cu_1/C_3N_4 and 1 mg•mL^{-1} CNT dispersed solutions were first prepared by sonication. And then, the two dispersions were mixed by equal volume to form Cu_1/C_3N_4/CNT dispersion for electrode modification. C_3N_4/CNT dispersion were prepared similarly with C_3N_4 replacing Cu_1/C_3N_4.

Characterization. XRD patterns of samples were recorded by a Rigaku RU-200b with Cu Kα radiation (λ = 0.15406 nm). SEM images were recorded on a Hitachi SU8020 to acquire the morphology of the catalysts. TEM images were performed on a Hitachi-7800 at 100.0 kV. HAADF-STEM tests were carried out by using a Titan 80-300 scanning/transmission electron microscope at 300 kV with a spherical aberration corrector. Nitrogen

adsorption–desorption isotherms were recorded on a Quadrasorb SI-MP system at 77 K. X-ray photoelectron spectra were gained from an ESCALab220i-XL electron spectrometer with an Al Kα radiation used. Fourier transform infrared (FT-IR) spectra were recorded on a Shimadzu IR Prestige-21 spectrometer.

XAFS measurement. The XAFS spectra at Cu K edge (E_0 = 8979 eV) was tested at beamline 14W1 station of Shanghai Synchrotron Radiation Facility worked at 3.5 GeV with an average current of 260 mA under "top-up" mode. The XAFS data were extracted in a fluorescence mode with Si (111) double-crystal monochromator and Lytle-type ion chamber, using Cu foil, Cu phthalocyanine and CuO as references. Program ATHENA in the IFEFFIT software packages was used for data analysis.

Electrochemical measurements. Electrochemical tests were performed on a CHI 760E electrochemical workstation with a three-electrode system in aCSF. A glassy carbon (GC) electrode (3 mm in diameter) modified with the catalyst was served as the working electrode, an Ag/AgCl electrode and a Pt wire were used as reference and counter electrode, respectively. Cyclic voltammetry (CV) experiments were performed in aCSF with a scan rate of 50 $mV \cdot s^{-1}$. Electrochemical impedance spectra (EIS) were recorded on an Autolab PGSTAT302 from 0.1 MHz to 0.1 Hz with a three-electrode system in aCSF.

Carbon fiber microelectrode (CFE) was fabricated as reported previously.[2] A single carbon fiber (7 μm diameter, Tokai Carbon Co., Tokai, Japan) was carefully inserted into the capillary, pulled on a vertical pipet puller (WD-1, Sichuan, China). Prior to modification, the fabricated CFE was sequentially sonicated in a solution of acetone, 3 M HNO_3, 1.0 M KOH, and deionized water for 3 min. Then the electrodes were subjected to electrochemical activation, first with potential-controlled amperometry at +2.0 V for 30 s and at -1.0 V for 10 s, and then with cyclic voltammetry in 0.5 M H_2SO_4 within a potential range from 0 to 1.0 V at a scan rate of 0.1 $V \cdot s^{-1}$ until a stable cyclic voltammogram was obtained.

In vivo experiments. In vivo experiments were performed as reported previously.[2] All in vivo experimental procedures were complied with the guidelines of the Animal Advisory Committee at the State Key Laboratory of Cognitive Neuroscience and Learning, and were approved by the Institutional Animal Care and Use Committee at Beijing Normal University. Adult male guinea pigs (250-300 g) used in this study were purchased from Health Science Center, Peking University. Briefly, the Cu_1/C_3N_4/CNT/CFE was inserted into the right cortex (AP = 3 mm, L = 2 mm lateral from bregma, V = 1 mm from surface of skull) according to the stereotaxic procedures. The microsized Ag/AgCl reference electrode was positioned into the dura of brain. Platinum wire was used as the counter electrode inserted in subcutaneous tissue on the brain. Exogenous aCSF containing 100 μM H_2O_2, MCS or GSOEt was microinfused to the local area of the microelectrode in the brain through silica capillary tube (4 cm length, 50 μm i.d., 375 μm o.d.) which was implanted into the right cortex parallel with Cu_1/C_3N_4/CNT/CFE, also denoted as SAC-based microsensor. These solutions were delivered from gas-impermeable syringes and pumped through tetrafluoroethylenehexafluoropropene (FEP) tubing by a microinjection pump (CMA100, CMA Microdialysis AB, Stockholm, Sweden). All local microinfusions were performed in the striatum of the rat brain at

the rate of 1.0 μL·min^{-1}.

2. Supplementary Figures and Tables

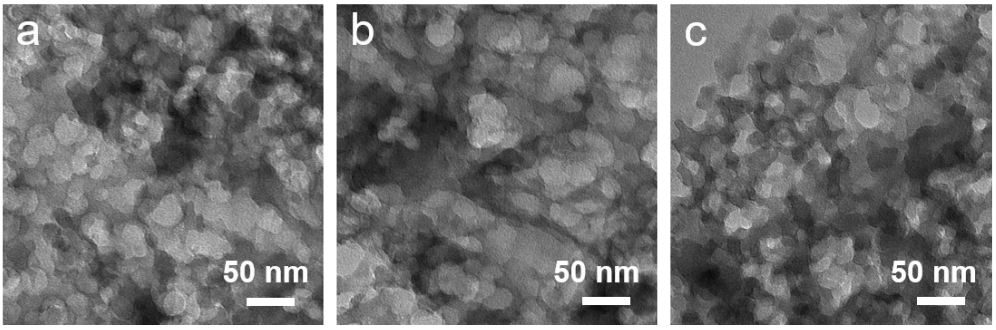

Fig. S1 TEM images of Fe_1/C_3N_4 (a), Co_1/C_3N_4 (b), Mn_1/C_3N_4 (c).

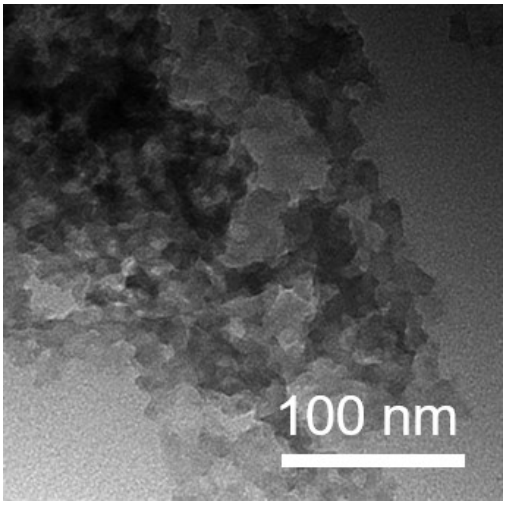

Fig. S2 TEM image of C_3N_4.

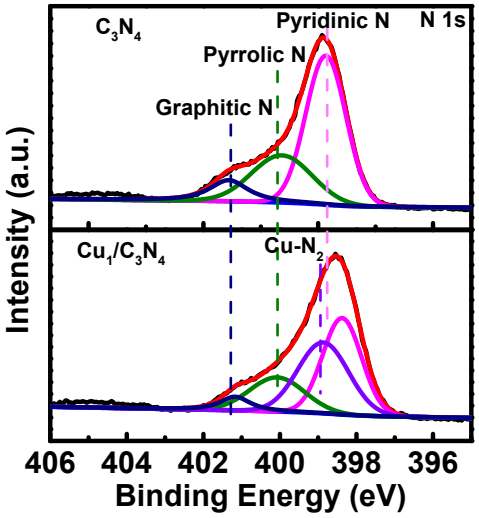

Fig. S3 High resolution N 1s XPS spectra of C_3N_4 and Cu_1/C_3N_4.

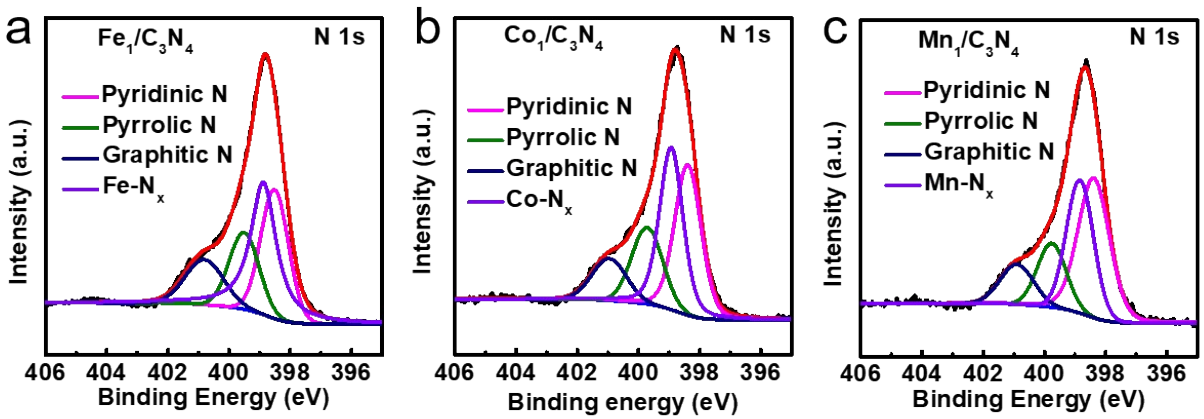

Fig. S4 High resolution N 1s XPS spectra of Fe_1/C_3N_4 (a), Co_1/C_3N_4 (b) and Mn_1/C_3N_4 (c).

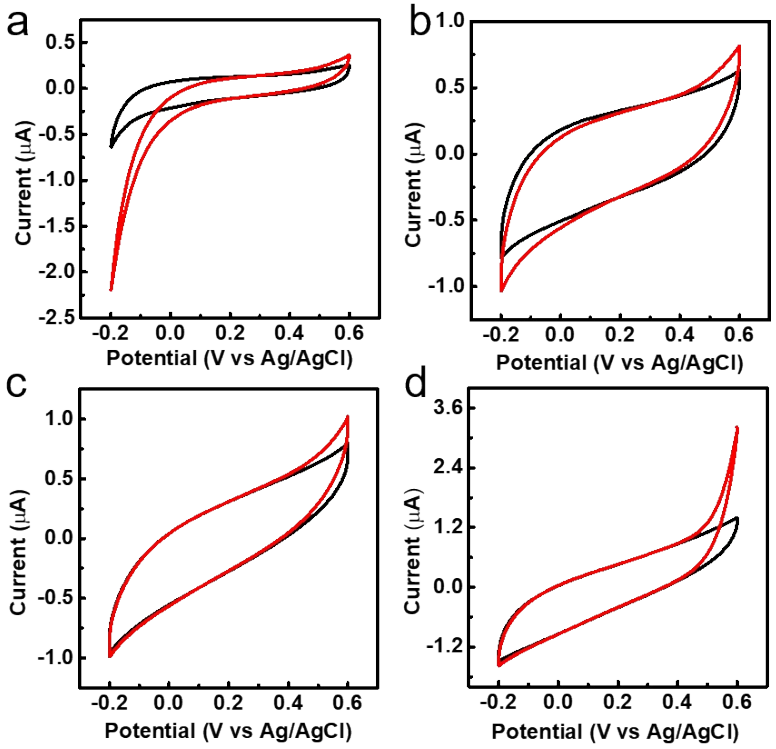

Fig. S5 CVs of Cu_1/C_3N_4/GC (a), Fe_1/C_3N_4/GC (b), Co_1/C_3N_4/GC (c) and Mn_1/C_3N_4/GC (d) in aCSF without (black line) and with (red line) 5 mM H_2O_2. Scan rates: 50 mV/s.

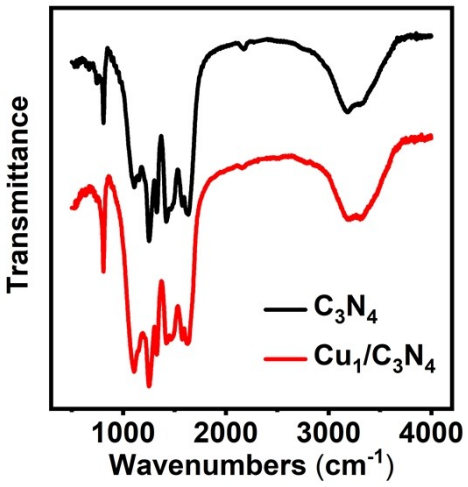

Fig. S6 Fourier transform infrared (FT-IR) spectra of the as-synthesized C_3N_4 (black line) and Cu_1/C_3N_4 (red line).

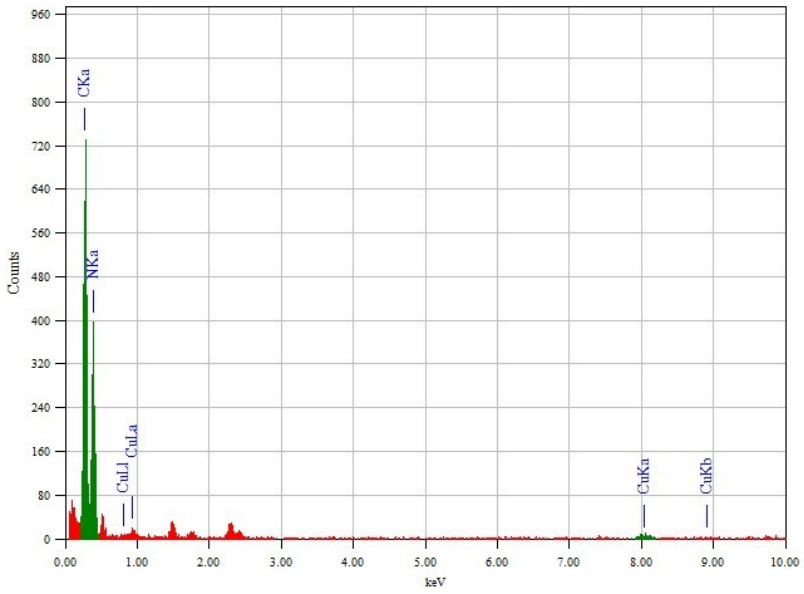

Fig. S7. The EDS spectrum recorded from the mapping region of Cu_1/C_3N_4 in Fig. 1c.

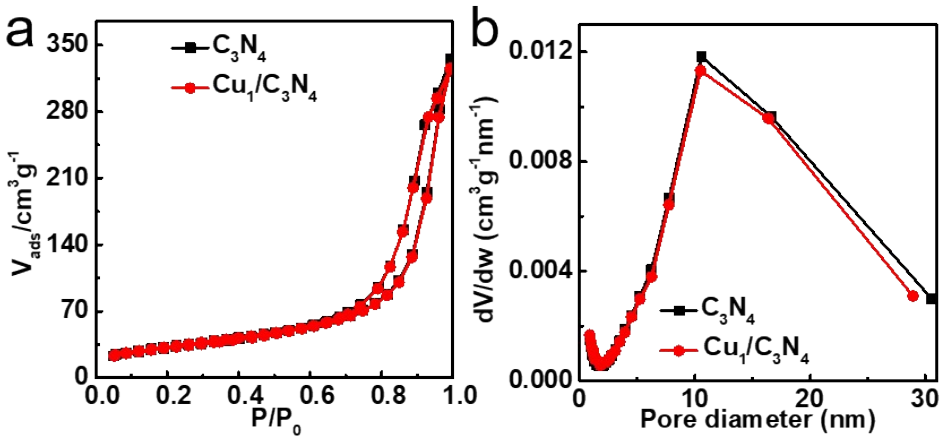

Fig. S8 Adsorption-desorption isotherms (a) and the pore size distribution plots (b) of C_3N_4 (black line) and Cu_1/C_3N_4 (red line).

Table S1. BET surface areas and pore sizes of C_3N_4 and Cu_1/C_3N_4.

Samples	S_{BET} (m^2/g)	Pore size (nm)
C_3N_4	**117.4283**	**8.9535**
Cu_1/C_3N_4	**117.3434**	**8.6964**

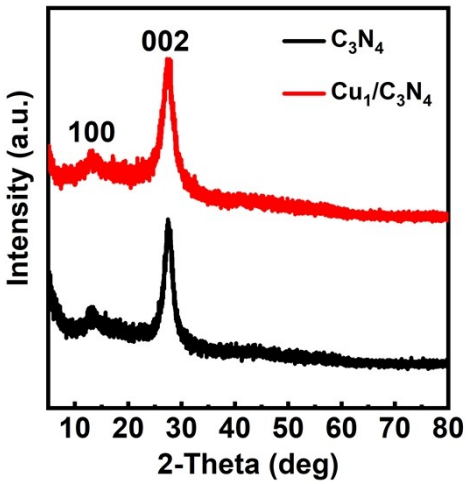

Fig. S9 XRD patterns of C_3N_4 (black line) and Cu_1/C_3N_4 (red line).

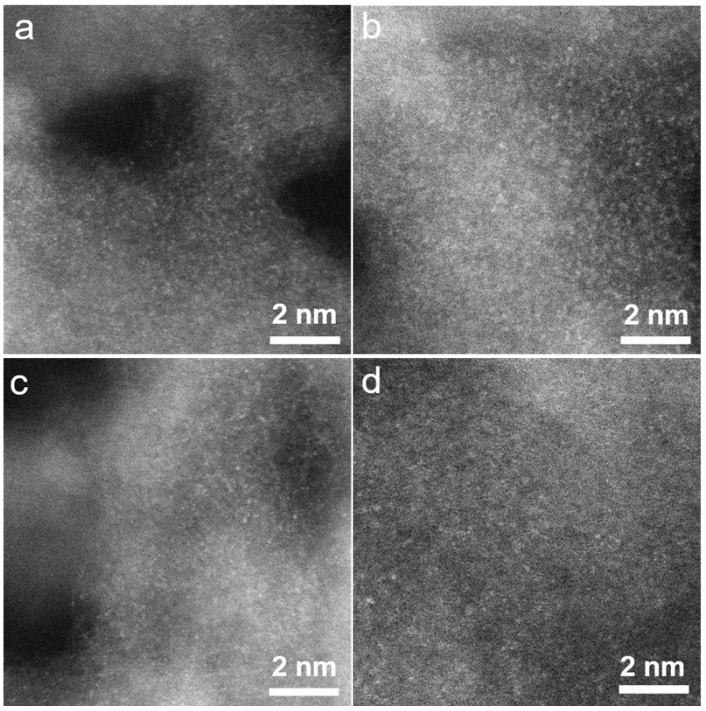

Fig. S10 Representative AC HAADF-STEM images of Cu_1/C_3N_4 at different regions.

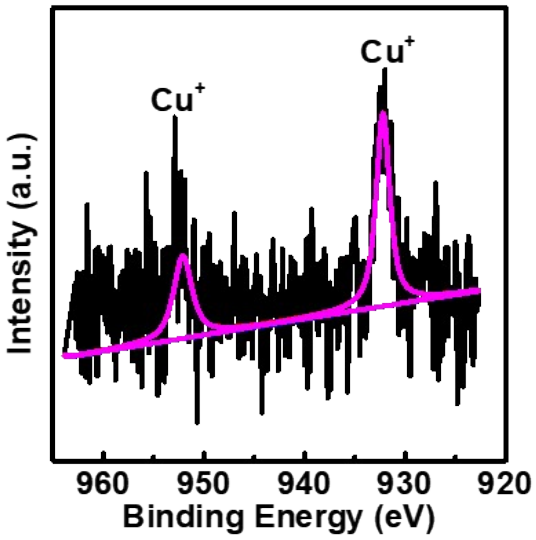

Fig. S11 High resolution Cu 2p XPS spectrum of Cu_1/C_3N_4.

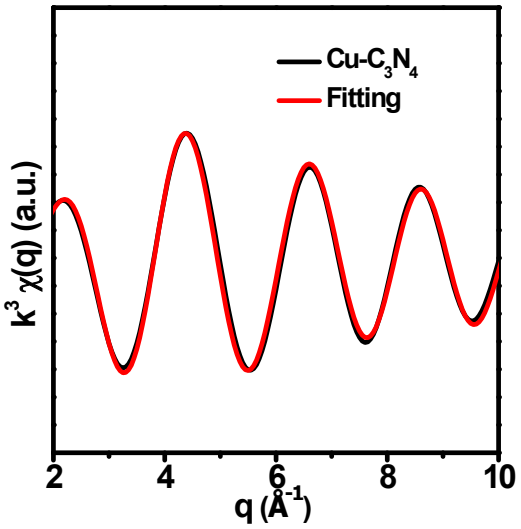

Fig. S12 Corresponding fitting curves of EXAFS spectrum of Cu_1/C_3N_4 in q space.

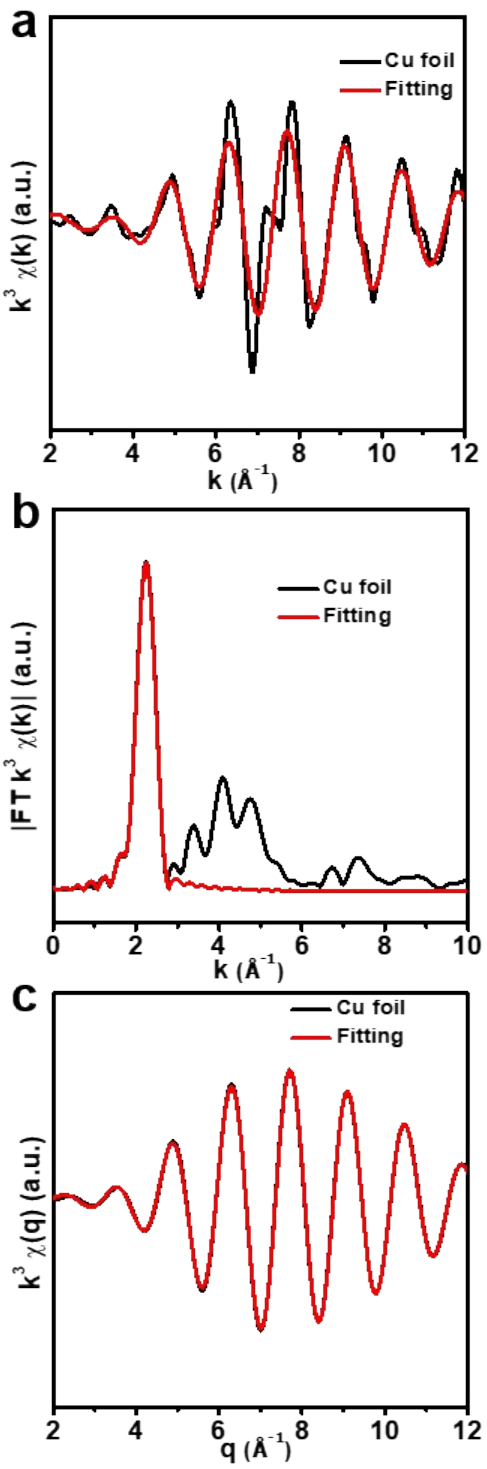

Fig. S13 The corresponding Cu foil EXAFS fitting curves at R space (a), k space (b) and q space (c).

Table S2. Structural parameters extracted from the Cu K-edge EXAFS fitting. ($S_0^2 = 0.81$)

Sample	Scattering pair	CN	R (Å)	σ^2 (10^{-3}Å^2)	ΔE_0 (eV)	R factor
Cu_1/C_3N_4	Cu-N/C	2.2	1.97	5.4	1.5	0.005
Cu foil	Cu-Cu	12*	2.54	4.0	0.5	0.004

S_0^2 is the amplitude reduction factor; CN is the coordination number; R is interatomic distance (the bond length between central atoms and surrounding coordination atoms); σ^2 is Debye-Waller factor (a measure of thermal and static disorder in absorber-scatterer distances); ΔE_0 is edge-energy shift (the difference between the zero kinetic energy value of the sample and that of the theoretical model). R factor is used to value the goodness of the fitting.

* This value was fixed during EXAFS fitting, based on the known structure.

Error bounds that characterize the structural parameters obtained by EXAFS spectroscopy were estimated as N ± 20%; R ± 1%; σ^2 ± 20%; ΔE_0 ± 20%.

Cu_1/C_3N_4 (FT range: 2.0-12.0 Å^{-1}; fitting range: 0.8-2.0 Å)

Cu foil (FT range: 2.0-12.0 Å^{-1}; fitting range: 1.4-2.8 Å)

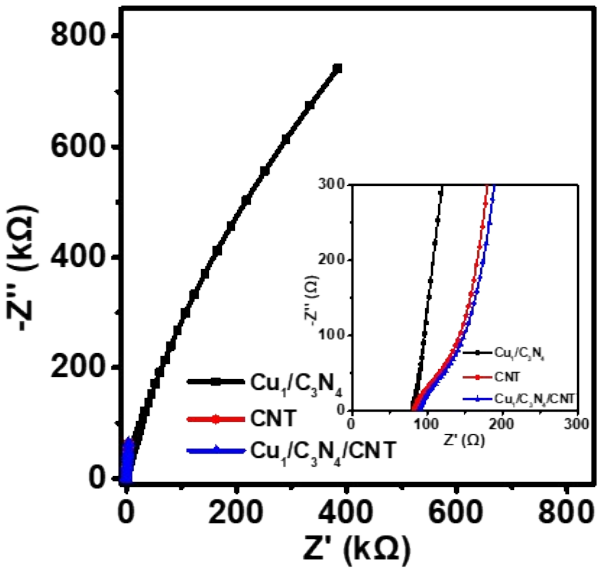

Fig. S14 Nyquist plots of electrochemical impedance spectra for GC electrodes modified with Cu_1/C_3N_4 (black line), CNT (red line), and Cu_1/C_3N_4/CNT (blue line) catalysts in aCSF under N_2 atmosphere operated at open circuit potential with an amplitude of 10 mV and a frequency range of 0.1 Hz – 100 kHz. Inset: the enlarged Nyquist plots.

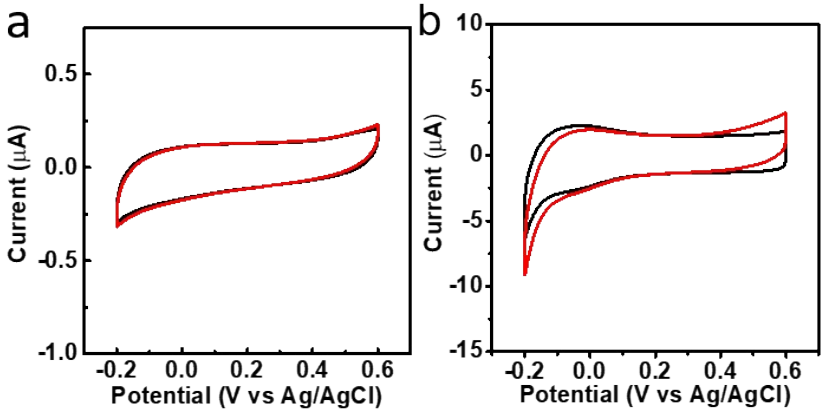

Fig. S15 CVs of C_3N_4/GC (a) and C_3N_4/CNT/GC (b) in aCSF without (black line) and with (red line) 5 mM H_2O_2. Scan rates: 50 mV/s.

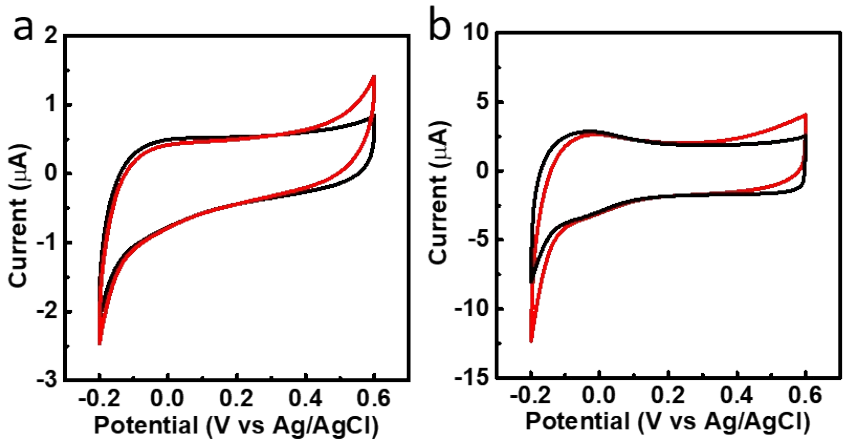

Fig. S16 CVs of bare GC (a) and CNT/GC (b) in aCSF without (black line) and with (red line) 5 mM H_2O_2. Scan rates: 50 mV/s.

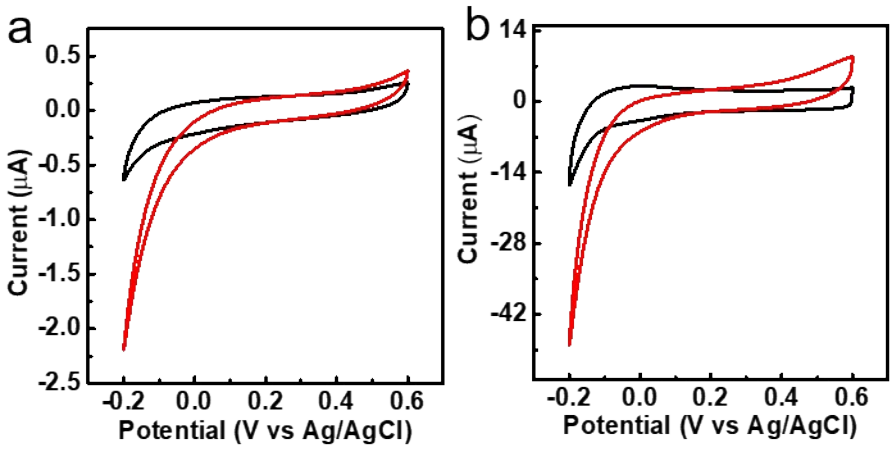

Fig. S17 CVs of Cu_1/C_3N_4/GC (a) and Cu_1/C_3N_4/CNT/GC (b) in aCSF without (black line) and with (red line) 5 mM H_2O_2. Scan rates: 50 mV/s.

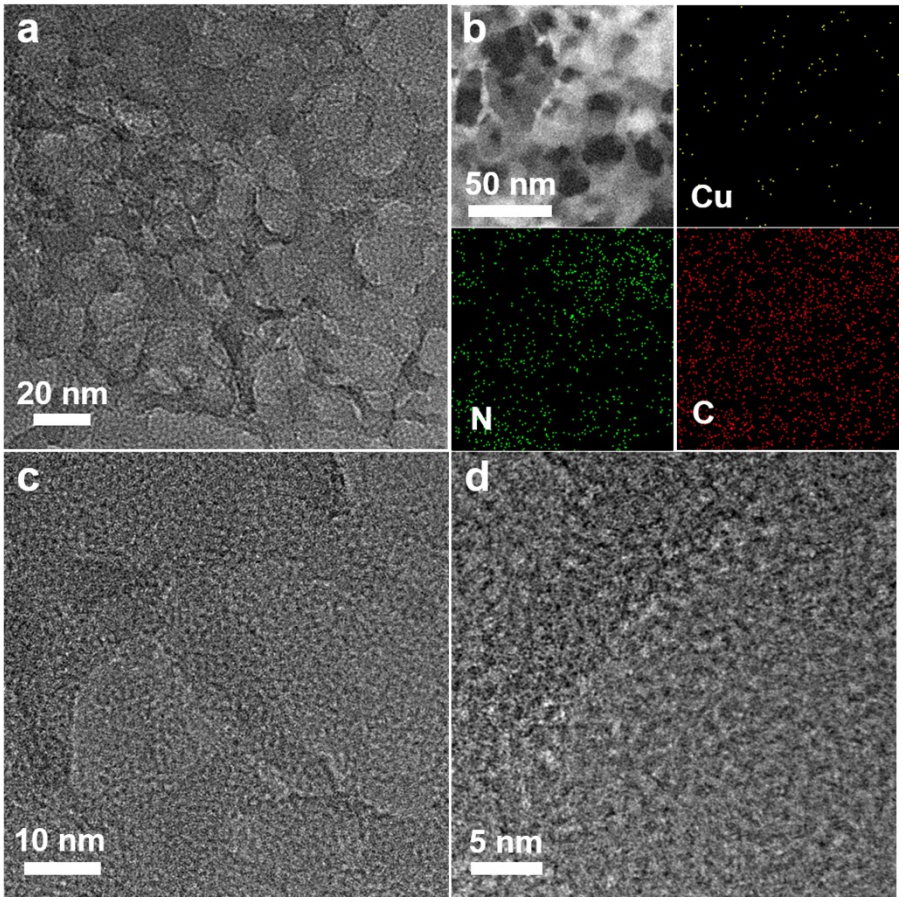

Figure S18. (a) TEM image of the Cu_1/C_3N_4 catalyst after test. (b) HAADF-STEM and corresponding element mapping images of the Cu_1/C_3N_4 catalyst after test showing the uniform distribution of Cu (yellow), N (green) and C (red). (c, d) High-resolution TEM images of the Cu_1/C3N4 catalyst after test.

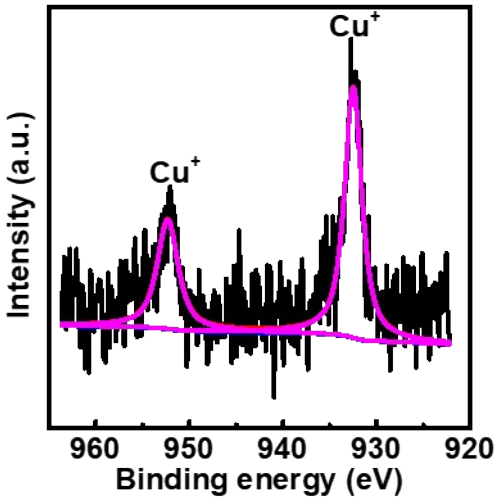

Fig. S19 High resolution Cu 2p XPS spectrum of the used Cu_1/C_3N_4.

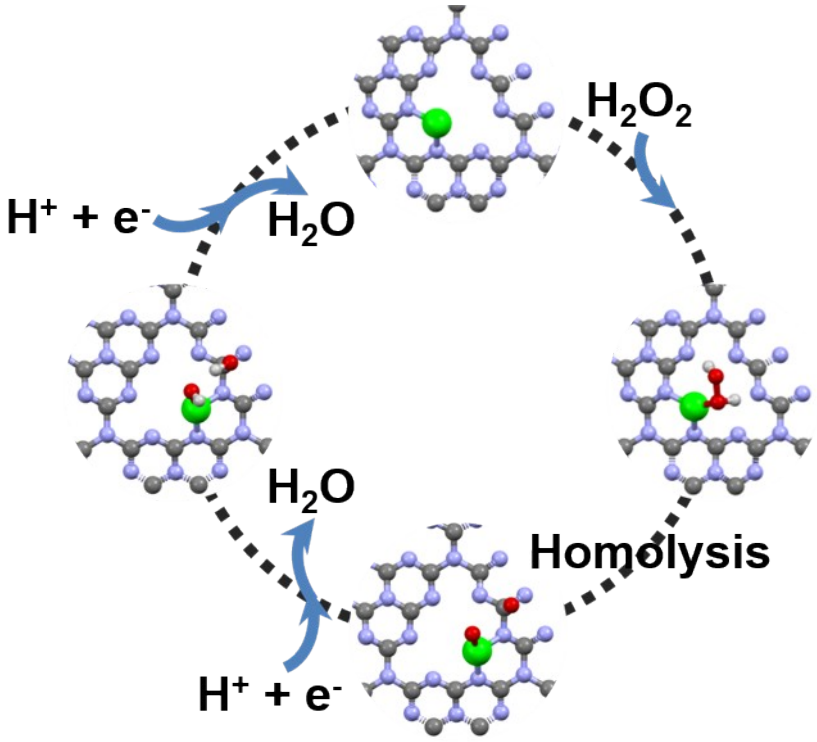

Fig. S20 Top views of atomic configurations for intermediate states of H_2O_2 reduction. Blue, black, green, red and grey spheres represent N, C, Cu, O and H atoms, respectively.

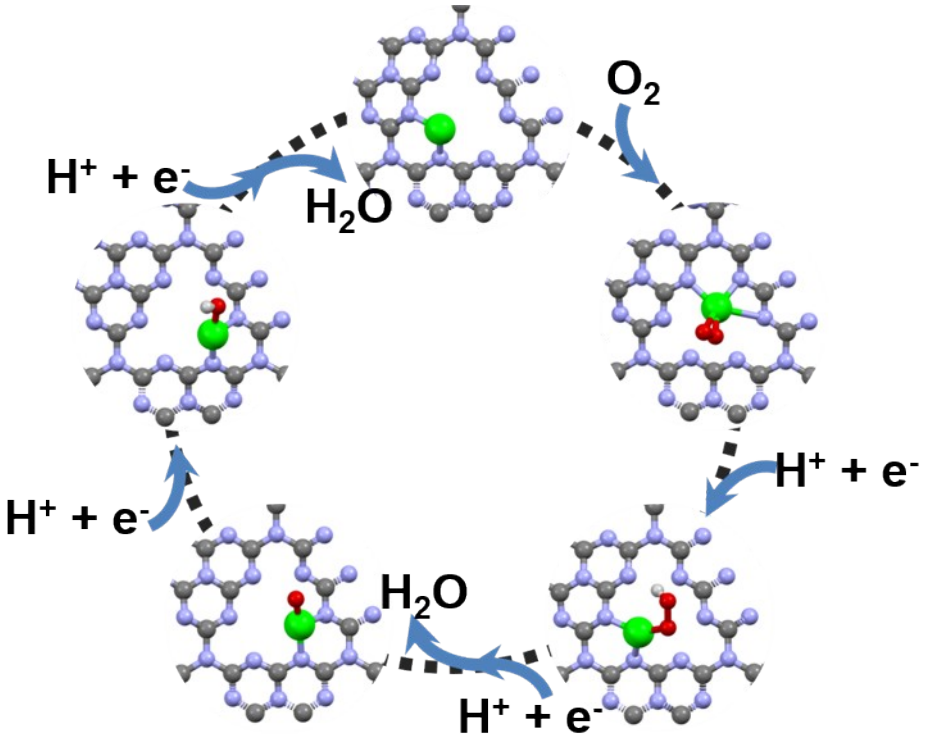

Fig. S21 Top views of atomic configurations for intermediate states of O_2 reduction. Blue, black, green, red and grey spheres represent N, C, Cu, O and H atoms, respectively.

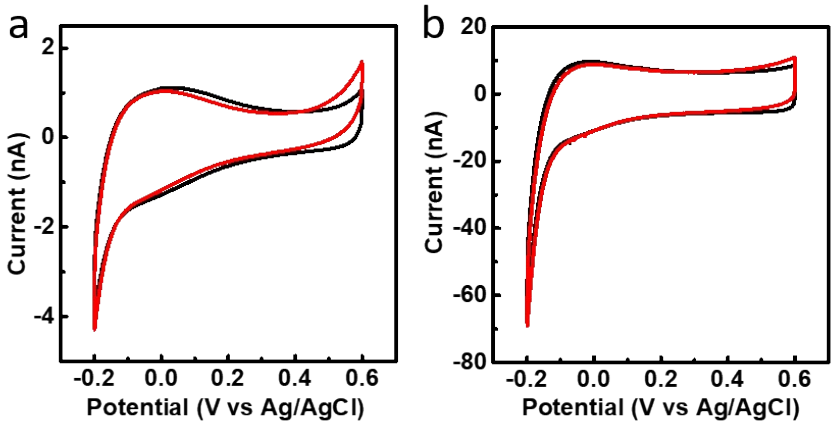

Fig. S22 CVs obtained with bare CFE (a) and CNT/CFE (b) in aCSF in the absence (black line) and presence of 5 mM H_2O_2 (red line). Scan rates: 50 mV/s.

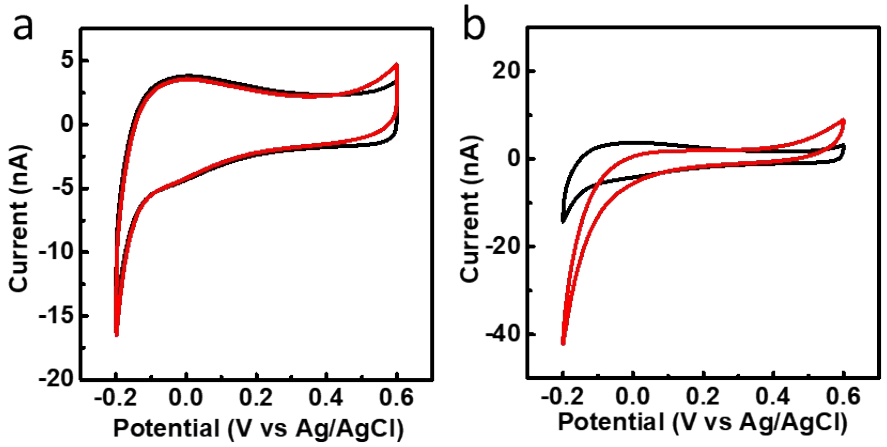

Fig. S23 CVs obtained with C_3N_4/CNT/CFE (a) and Cu_1/C_3N_4/CNT/CFE (b) in aCSF in the absence (black line) and presence of 5 mM H_2O_2 (red line). Scan rates: 50 mV/s.

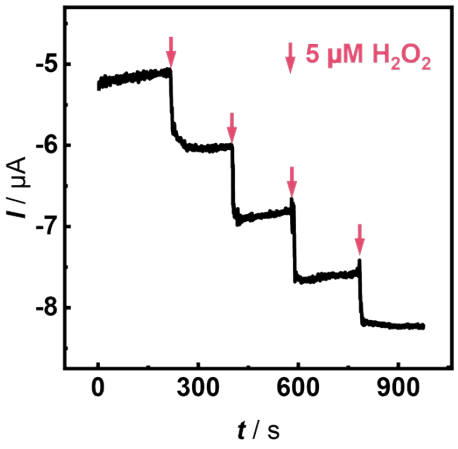

Fig. S24 Amperometric response at the microsensor in aCSF toward successive addition of 5 μM H_2O_2. Applied potential: 0.0 V *vs*. Ag/AgCl.

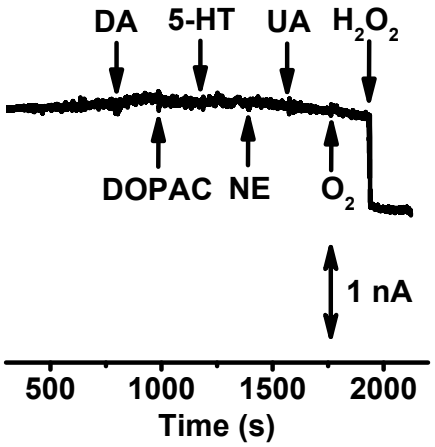

Fig. S25 Amperometric response recorded with the microsensor in aCSF toward 10 µM DA, 10 µM DOPAC, 10 µM 5-HT, 10 µM NE, 10 µM UA, 50 µM O_2 and 5 µM H_2O_2. Applied potential: 0.0 V *vs*. Ag/AgCl.

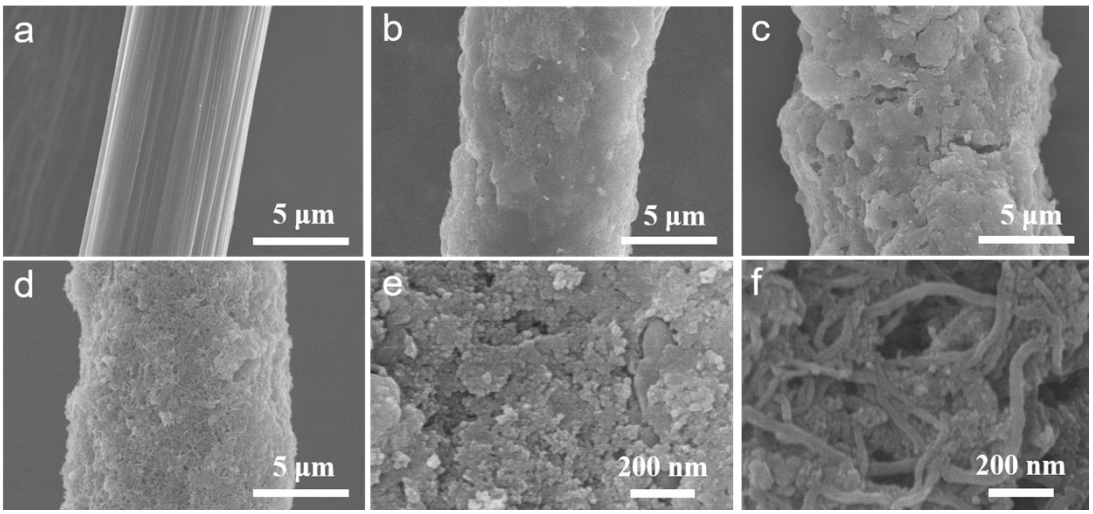

Fig. S26 (a-d) SEM images of bare CFE (a), C_3N_4/CFE (b), Cu_1/C_3N_4/CFE (c) and Cu_1/C_3N_4/CNTs/CFE (d). (e-f) The magnified images of (c) and (d), respectively.

Compared to bare CFE with relatively smooth surface (Fig. S24a), the microsensor prepared with the nanocomposites of Cu_1/C_3N_4 and CNTs displays a rough surface but with the uniform coating of the catalyst (Fig. S24b-f).

3. Supplementary Discussions of Calculations

All the calculations in this work were performed by spin-polarized DFT with a periodic surface model using CASTEP program implemented in the Materials Studio. The OTFG (on the fly generated) ultrasoft pseudopotentials and the Perdew-Burke-Ernzerhof exchange-correlation functional within the generalized gradient approximation were selected[3]. A cut-off energy of 500 eV was used for plane wave basis set, while further increasing the value causes little difference in the results (Figure S27). A Monkhorst-Pack k-point 0.03 $Å^{-1}$ spacing was utilized to integrate Brillouin zone. A quasi-Newton optimized BFGS (Broyden, Fletcher, Goldfarb, and Shanno) algorithm was used to optimize the adsorption geometries. The convergence criteria for the total energy, forces, stress, atomic displacement, and self-consistent field iterations were set to 1×10^{-5} eV $atom^{-1}$, 3×10^{-2} eV $Å^{-1}$, 5×10^{-2} GPa, 1×10^{-3} Å, and 1×10^{-6} eV $atom^{-1}$, respectively.

The reaction energy (ΔE) of each elementary step was calculated using:

$$\Delta E = \sum E_{\text{products}} - \sum E_{\text{reactants}}$$

$\sum E_{\text{reactants}}$ and $\sum E_{\text{products}}$ are the total energy of the reactants and product, respectively.

The ORR and HPRR reaction pathways were calculated on Cu_1/mpg-C_3N_4 model. The computational hydrogen electrode was utilized to obtain free energies for each state. In neutral condition, the $4e^-$ ORR could go through a following pathway with several elementary steps:

$$O_2 + * \rightarrow O_2*$$

$$O_2* + H^+ + e^- \rightarrow OOH*$$

$$OOH* + H^+ + e^- \rightarrow O* + H_2O$$

$$O* + H^+ + e^- \rightarrow OH*$$

$$OH* + H^+ + e^- \rightarrow H_2O + *$$

And the HPRR pathway consists of following steps:

$$H_2O_2 + * \rightarrow H_2O_2*$$

$$H_2O_2^* \rightarrow 2OH^*$$

$$2OH^* + H^+ + e^- \rightarrow H_2O + OH^*$$

$$OH^* + H^+ + e^- \rightarrow H_2O + *$$

The chemical potential for ($H^+ + e^-$) (i.e. the free energy of each H) is equal to that of *1/2* H_2 when setting the reference potential to be that of the standard hydrogen electrode at standard condition (T = 298 K, P_{H2}=1 bar, and pH=0). The change of reaction free energy (ΔG) is further estimated by the function:

$$\Delta G = \Delta H - T\Delta S - qU + k_B T \ln 10 \times \mathrm{pH}$$

Δ*H*: the reaction enthalpy of each elementary step and is obtained from the reaction energy (Δ*E*) by calculations using zero-point energy (ZPE) correction

Δ*S*: the change of entropy at temperature *T*

U: the applied potential

q: the charge transferred in each elementary step

k_B: the Boltzmann constant.

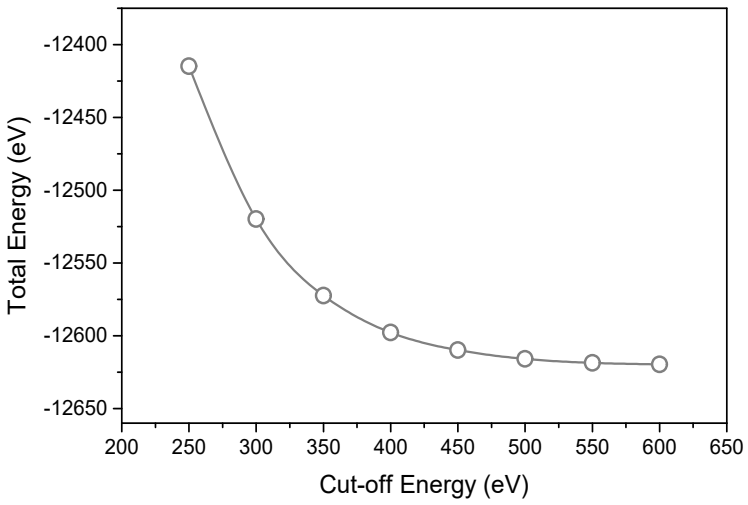

Fig. S27 Total DFT energy varies with the cut-off energy for the periodic surface model used in this work.

Table S3. Calculated Gibbs free energies (ΔG) of elementary steps for H_2O_2 reduction and O_2 reduction on Cu_1/C_3N_4 SAC.

Elementary reactions		**ΔG (eV)**
H_2O_2 reduction	$H_2O_2 + * \rightarrow H_2O_2*$	-2.326
	$H_2O_2* \rightarrow 2OH*$	-1.798
	$2OH* + H^+ + e^- \rightarrow H_2O + OH*$	-0.505
	$OH* + H^+ + e^- \rightarrow H_2O + *$	1.31
O_2 reduction	$O_2 + * \rightarrow O_2*$	-1.933
	$O_2* + H^+ + e^- \rightarrow OOH*$	-0.862
	$OOH* + H^+ + e^- \rightarrow O* + H_2O$	-0.933
	$O* + H^+ + e^- \rightarrow OH*$	-1.999
	$OH* + H^+ + e^- \rightarrow H_2O + *$	1.44

4. References

[1] A. Savateev, N. V. Tarakina, V. Strauss, T. Hussain, K. Brummelhuis, J. M. S. Vadillo, Y. Markushyna, S. Mazzanti, A. P. Tyutyunnik, R. Walczak, M. Oschatz, D. M. Guldi, A. Karton, M. Antonietti, *Angew. Chem. Int. Ed.* **2020**, *59*, 15061-15068.

[2] F. Wu, C. Pan, C.-T. He, Y. Han, W. Ma, H. Wei, W. Ji, W. Chen, J. Mao, P. Yu, D. Wang, L. Mao, Y. Li, *J. Am. Chem. Soc.* **2020**, *142*, 16861-16867.

[3] B. Hammer, L. B. Hansen, J. K. Nørskov, *Phys. Rev. B: Condens. Matter Mater. Phys.* **1999**, *59*, 7413−7421.